2D anisotropic complex-Padé finite-difference depth migration

D. Amazonas[1], R. Aleixo[2], J. Schleicher[2] and J. Costa[1], [1]Federal University of Pará and [2]University of Campinas

ABSTRACT

Standard real-valued finite-difference (FD) and Fourier finite-difference (FFD) migrations cannot handle evanescent waves correctly, which can lead to numerical instabilities in the presence of strong velocity variations. A possible solution to these problems is the complex Padé approximation, which avoids problems with evanescent waves by a rotation of the branch cut. In this paper, we apply this approximation to the acoustic wave equation for vertical transversely anisotropic (VTI) media to derive a more stable FD migration for such media. Our studies of the dispersion relation of the new method indicate that it should provide more stable migration results with less artifacts and higher accuracy at steep dips. The best rotation angle of the branch cut turns out to be 60°. This result is confirmed by the numerical impulse responses.

INTRODUCTION

Wave-equation migration algorithms have performed better than ray-based migration methods when the velocity model has strong lateral velocity variations. One drawback of wave-equation migrations, though, is their general difficulty to image steep dips. However, recent advances, particularly for finite-difference (FD) (Claerbout, 1971) and Fourier finite-difference (FFD) migrations (Ristow and Rühl, 1994) can provide wide-angle approximations for the one-way continuation operators, thus improving the imaging of steep-dip reflectors.

However, standard real-valued FD and FFD migrations cannot handle evanescent waves correctly (Millinazzo et al., 1997). As a consequence, FFD algorithms tend to become numerically unstable in the presence of strong velocity variations (Biondi, 2002). To overcome this limitation, Biondi (2002) proposes an unconditionally stable extension for the FFD algorithm. Earlier, Millinazzo et al. (1997) proposed a different approach to treating these evanescent modes in ocean acoustic applications, introducing an extension of the Padé approximation called complex Padé. The complex Padé expansion has been used in applied geophysics. Zhang et al. (2003) use the method in finite-difference migration. However, their implementation is not optimized for wide angles. Zhang et al. (2004) propose an FFD migration based on a different realization of complex Padé. Recently, Amazonas et al. (2007) derived FD and FFD algorithms using the complex Padé approximation for isotropic media to handle evanescent waves. They demonstrated that this procedure stabilizes FD and FFD migration without requiring special treatment for the migration domain boundaries and enables an accurate migration up to higher dips.

In anisotropic media, the acoustic wave equation does not describe physically realizable phenomena, because acoustic media cannot be anisotropic. Thus, Alkhalifah (1998) used the dispersion relationship for vertical transversely isotropic (VTI) media to derive a acoustic wave equation for VTI media. Based on his work, several authors have developed FD and FFD migration methods in VTI media (Ristow, 1999; Han and Wu, 2005; Nolte, 2005; Zhang et al., 2005). Fei and Liner (2008) proposed a hybrid FFD and FD algorithm for VTI media. In this paper, we combine the ideas of these authors with the complex Padé approximation to derive a more stable FD algorithm for VTI media.

METHOD

According to Alkhalifah (2000), the acoustic wave equation for VTI media is given by

$$\frac{\partial^2 P}{\partial t^2} = (1+2\eta)v_n^2\frac{\partial^2 P}{\partial x^2} + v_{p0}^2\frac{\partial^2 P}{\partial z^2} - 2\eta v_n^2 v_{p0}^2\frac{\partial^4 F}{\partial x^2 \partial z^2}, \quad (1)$$

where

$$F(x,z,t) = \int_0^t \int_0^{t'} P(x,z,\tau)d\tau\, dt'. \quad (2)$$

Applying the Fourier transform in x, z and t to equation (1), we obtain the following dispersion relation

$$k_z^2 = \frac{v_n^2}{v_{p0}^2}\left(\frac{\omega^2}{v_n^2} - \frac{\omega^2\, k_x^2}{\omega^2 - 2\eta v_n^2\, k_x^2}\right), \quad (3)$$

where k_x is the horizontal wavenumber, ω is frequency, v_{p0} is the vertical P-wave velocity of the medium and v_n is the NMO velocity, given by

$$v_n = v_{p0}\sqrt{1+2\delta}. \quad (4)$$

Moreover, parameter η is given by

$$\eta = \frac{\epsilon - \delta}{1+2\delta}, \quad (5)$$

where ϵ and δ are Thomsen's parameters (Thomsen, 1986).

From Fei and Liner (2008), we use the following notation

$$u^2 = \frac{k_x^2\, v_n^2}{\omega^2}. \tag{6}$$

Taking the square root of equation (3) using equation (6) yields

$$k_z = \frac{\omega}{v_{p0}} \sqrt{1 - \frac{u^2}{1 - 2\eta\, u^2}}. \tag{7}$$

In analogy to the small dip-angle approximation of the corresponding isotropic expression (Ristow and Rühl, 1994), the square root in equation (7) can also be expanded into a Taylor series at point $u = 0$ Fei and Liner (2008). This leads to

$$k_z = 1 - \frac{1}{2}u^2 - \frac{g_2}{8}u^4 - \frac{g_3}{16}u^6, \tag{8}$$

where

$$g_2 = 1 + 8\eta, \tag{9}$$

$$g_3 = 1 + 8\eta + 32\eta^2. \tag{10}$$

Note that setting $\eta = 0$, i.e., $g_1 = g_2 = 1$ in these equations provides an approximation for elliptically anisotropic or isotropic media.

COMPLEX PADÉ FD APPROXIMATION

In this section, we derive the complex Padé approximation to the above dispersion relation, because we want a steep-dip approximation and improved stability by better handling of evanescent waves. For this purpose, we have to represent the square-root in equation (7) in the complex Padé expansion.

Real Padé approximation

A formal representation for square-root operator is based on the Padé expansion (Bamberger et al., 1988):

$$\sqrt{1 - X^2} \approx 1 - \sum_{n=1}^{N} \frac{a_n\, X^2}{1 - b_n\, X^2}, \tag{11}$$

where for our anisotropic k_z of equation (7),

$$X^2 = \frac{u^2}{1 - 2\eta\, u^2}. \tag{12}$$

The number of terms N of the expansion should, in principle, be infinite, but in practice, generally two to four terms suffice for a reasonable approximation. The coefficients a_n and b_n are (Bamberger et al., 1988):

$$a_n = \frac{2}{2N+1} \sin^2 \frac{n\,\pi}{2N+1}, \tag{13}$$

$$b_n = \cos^2 \frac{n\,\pi}{2N+1}. \tag{14}$$

Complex Padé approximation

If $X^2 > 1$ in equation (11), the left side is a purely imaginary number, but the right side remains a real-valued quantity. In other words, the approximation breaks down. Physically, this means that approximation (11) cannot properly handle evanescent modes. This causes numerical instabilities and is responsible for the unstable behavior of the FFD algorithm in the presence of strong velocity variations (Biondi, 2002).

To overcome these limitations, Millinazzo et al. (1997) propose a complex representation of the Padé expansion in equation (11). They achieve this goal by rotating the branch cut of the square root in the complex plane. Their final expression is

$$\sqrt{1 - X^2} \approx C_0 - \sum_{n=1}^{N} \frac{A_n\, X^2}{1 - B_n\, X^2}, \tag{15}$$

where,

$$A_n = \frac{a_n e^{-i\alpha/2}}{[1 + b_n(e^{-i\alpha} - 1)]^2}, \tag{16}$$

$$B_n = \frac{b_n e^{-i\alpha}}{1 + b_n(e^{-i\alpha} - 1)}, \tag{17}$$

$$C_0 = e^{i\alpha/2} \left[1 + \sum_{n=1}^{N} \frac{a_n(e^{-i\alpha} - 1)}{1 + b_n(e^{-i\alpha} - 1)} \right], \tag{18}$$

with a_n and b_n as defined in equations (13) and (14), respectively. The values A_n and B_n are the complex Padé coefficients, and is the rotation angle of the branch cut of the square root in the complex plane.

Thus, expanding k_z of equation (7) into a complex Padé series, we find

$$k_z = \frac{\omega}{v_{p0}} \left[C_0 - \sum_{n=1}^{N} \frac{A_n\, X^2}{1 - B_n\, X^2} \right] \tag{19}$$

with X defined in equation (12). This is the *2D anisotropic complex-Padé finite-difference depth migration operator in VTI media*. Note that, as before, setting $\eta = 0$ in equation (12) leads to the corresponding operator for isotropic and elliptically anisotropic media.

To evaluate the quality of the complex Padé FD approximation (19), Figure 1 shows its comparison with the exact dispersion relation for a homogeneous medium. The FD approximation was calculated using the first three terms of the series with five different rotation angles of $\alpha = 5^\circ$, $\alpha = 45^\circ$, $\alpha = 60^\circ$, $\alpha = 75^\circ$, and $\alpha = 90^\circ$. The improvement in the approximation of the real part of the dispersion relation with increasing α is evident. The blessings are a bit more mixed for the imaginary part. While the approximation in the evanescent region improves for increasing α, there is a short interval of negative imaginary part immediately before the evanescent region, which increases with α. Note that this negative imaginary part will cause the evanescent waves to increase exponentially. For this reason, the best Padé FD approximation of the imaginary part is actually achieved for a rotation angle of about 60°. Since the main numerical instabilities of an FD migration are caused by incorrectly treated evanescent waves, it is to be expected

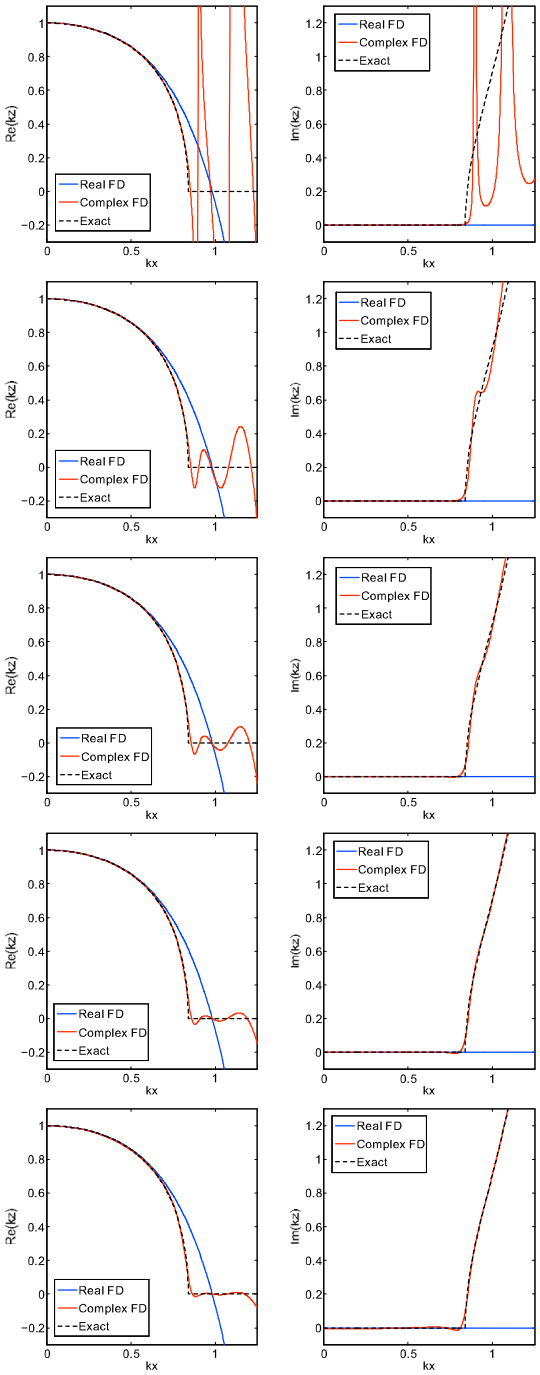

Figure 1: Complex Padé FD approximation for the dispersion relation of the one-way wave equation, computed with three terms and different rotation angles. First: $\alpha = 5^\circ$, Second: $\alpha = 45^\circ$, Third: $\alpha = 60^\circ$, Forth: $\alpha = 75^\circ$, Fifth $\alpha = 90^\circ$. Left: Real part. Right: Imaginary part.

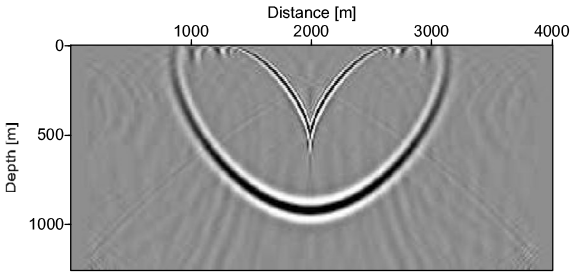

Figure 2: Real Padé ($\alpha = 0^\circ$) FD migration for an impulse response for a constant-velocity VTI medium. The anisotropy parameters are $\epsilon = 0.21$ and $\delta = -0.032$.

that a rotation angle of about 60° will produce the cleanest migrated image with the least artifacts. Note, however, that even a rotation by a small angle improves the behavior of the FD approximation (see top part of Figure 1). Although it creates rather strong fluctuation in the evanescent domain of the real part of k_z, it already introduces a nonzero imaginary part, meaning that the incorrect evanescent modes at least will be attenuated. In this respect, it is important to note that the peaks in the imaginary part, representing the strongest damping, coincide with peaks in the real part that indicate the most incorrect propagation behavior.

IMPULSE RESPONSE TEST

As a next step, we investigate the impulse response of the acoustic VTI wave equation (1). For this purpose, it is important to recognize that this equation has two solutions (Alkhalifah, 2000). One of these solutions is the desired result representing a wavefront coincident with the elastic compressional wavefront. The other solution is an additional event, which has previously been observed in full waveform modeling. However, apparently this additional event was not always understood as a second solution to the acoustic VTI wave equation. Therefore, it has been labeled as numerical artifact (Grechka et al., 2004), sometimes called the pseudo-S-wave artifact (Fei and Liner, 2008). Alkhalifah (2000) solved equation (1) analytically and observed that the undesired solution can be eliminated with proper initial conditions. However, such initial conditions would have to be medium dependent and are thus very hard to find.

The FD algorithm is a numerical simulation of the above VTI wave equation and therefore includes both solutions. Tests by Alkhalifah (2000) indicate that the second solution does not develop in isotropic regions. Thus, he suggests the use of isotropic layers to suppress it. Fei and Liner (2008) seek instead a more general algorithm that does not include the additional solution. They demonstrated that the event can be eliminated by a hybrid application of FFD and FD migrations. Here, we study pure FD migration and thus will have to accept the presence of the second event.

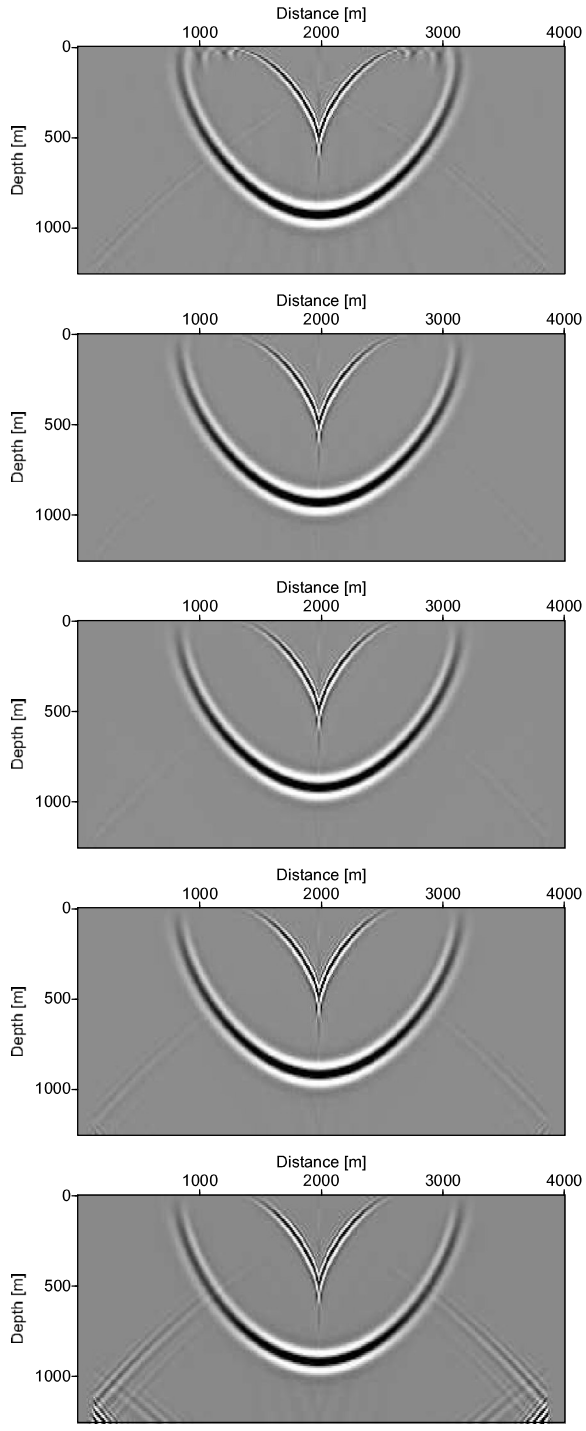

Figure 3: Complex Padé FD migration for an impulse response for a constant-velocity VTI medium. The anisotropy parameters are $\epsilon = 0.21$ and $\delta = -0.032$. First: $\alpha = 5^\circ$, Second: $\alpha = 45^\circ$, Third: $\alpha = 60^\circ$, Forth: $\alpha = 75^\circ$, Fifth $\alpha = 90^\circ$.

As a reference, Figure 2 shows the impulse response at $t = 0.5$ s of a real Padé ($\alpha = 0^\circ$) FD migration for a homogeneous (constant velocity, constant η) VTI medium. The source pulse is a Ricker pulse with peak frequency of 25 Hz. The migration was carried out using three terms in the Padé expansion.

Figure 3 depicts the same impulse response of the corresponding complex Padé FD migration in the same medium, using a rotation angle of $\alpha = 05^\circ$, $\alpha = 45^\circ$, $\alpha = 60^\circ$, $\alpha = 75^\circ$ and $\alpha = 90^\circ$, respectively.

The most prominent features in both figures are the two stronger events that are the two solutions of the acoustic VTI wave equation, i.e., the desired qP wavefront and the undesired pseudo-S wave. Additionally, we immediately recognize lots of numerical instabilities, even causing noncausal events in Figure 2. These are greatly reduced in all panels of Figure 3. Note in particular that even the rotation angle of 5° almost eliminates most of the noncausal events in spite of its rather poor approximation of the evanescent part of the dispersion relation.

As a final, more subtle difference between Figures 2 and 3, we note that while all impulse responses have energy up to high propagation angles, the real Padé approximation produces a slightly stronger distortion of the shape of the desired event at steep dips, causing it to bend inwards at the top. The improvement achieved by the complex Padé representation is a consequence of the better approximation of the dispersion relation in the high-angle range.

Comparing the complex Padé FD impulse responses of Figure 3 to each other, we observe that the image for $\alpha = 60^\circ$ is the best one. This is in agreement the previous study of the dispersion relations, which also indicates that $\alpha = 60^\circ$ is the best rotation angle for the complex Padé FD migration. Note that, for the other angles, the impulse responses also have a good shape, but in these image the remaining artifacts caused by incorrectly treated evanescent waves are stronger.

CONCLUSIONS

In this work, we have combined the anisotropic migration for VTI media using the acoustic VTI wave equation of Alkhalifah (2000) with the complex Padé FD approximation of Amazonas et al. (2007) to derive a more stable VTI migration method. Our studies of the dispersion relation of the new method indicate that it should provide more stable migration results with less artifacts and higher accuracy at steep dips. The best rotation angle of the branch cut turns out to be 60°. This result is confirmed by the numerical impulse responses.

ACKNOWLEDGMENTS

This work was kindly supported by the Brazilian research agencies CNPq and FAPESP (proc. 06/04410-5), as well as Petrobras and the sponsors of the *Wave Inversion Technology (WIT) Consortium*.

REFERENCES

Alkhalifah, T., 1998, Acoustic approximations for processing in transversely isotropic media: Geophysics, **63**, no. 2, 623–631.

Alkhalifah, T., 2000, An acoustic wave equation for anisotropic media: Geophysics, **65**, no. 4, 1239–1250.

Amazonas, D., Costa, J. C., Schleicher, J., and Pestana, R., 2007, Wide-angle FD and FFD migration using complex Padé approximations: Geophysics, **72**, no. 6, S215–S220.

Bamberger, A., Engquist, L. H., and Joly, P., 1988, Higher order paraxial wave equation approximations in heterogeneous media: J. Appl. Math., **48**, 129–154.

Biondi, B., 2002, Stable wide-angle Fourier finite-difference downward extrapolation of 3-D wavefields: Geophysics, **67**, no. 3, 872–882.

Claerbout, J. F., 1971, Toward a unified theory of reflector mapping: Geophysics, **36**, no. 3, 467–481.

Fei, T. W., and Liner, C. L., 2008, Hybrid Fourier finite-difference 3D depth migration for anisotropic media: Geophysics, **73**, no. 2, S27–S34.

Grechka, V., Zhang, L., and Rector III, J. W., 2004, Shear waves in acoustic anisotropic media: Geophysics, **69**, no. 2, 576–582.

Han, Q., and Wu, R.-S., 2005, A one-way dual-domain propagator for scalar qP-waves in VTI media: Geophysics, **70**, no. 2, D9–D17.

Millinazzo, F. A., Zala, C. A., and Brooke, G. H., 1997, Square-root approximations for parabolic equation algorithms: J. Acoust. Soc. Am., **101**, no. 2, 760–766.

Nolte, B., 2005, Converted-wave migration for VTI media using Fourier finite-difference depth extrapolation: EAGE, Expanded Abstracts, page P001.

Ristow, D., and Rühl, T., 1994, Fourier finite-difference migration: Geophysics, **59**, no. 12, 1882–1893.

Ristow, D., 1999, Migrations in transversely isotropic media using implicit finite-difference operators: Journal of Seismic Exploration, **8**, no. 1, 39–55.

Thomsen, L., 1986, Weak elastic anisotropy: Geophysics, **51**, no. 10, 1954–1966.

Zhang, L., Rector, J. W., and Hoversten, G. M., 2003, Split-step complex Padé migration: Journal of Seismic Exploration, **12**, 229–236.

Zhang, L., Rector, J. W., Hoversten, G. M., and Fomel, S., 2004, Split-step complex Padé-Fourier depth migration.: SEG Int'l Exposition and 74th Annual Meeting.

Zhang, L., Hua, B., and Calandra, H., 2005, 3D fourier finite difference anisotropic depth migration: SEG Technical Program Expanded Abstracts, **24**, no. 1, 1914–1917.